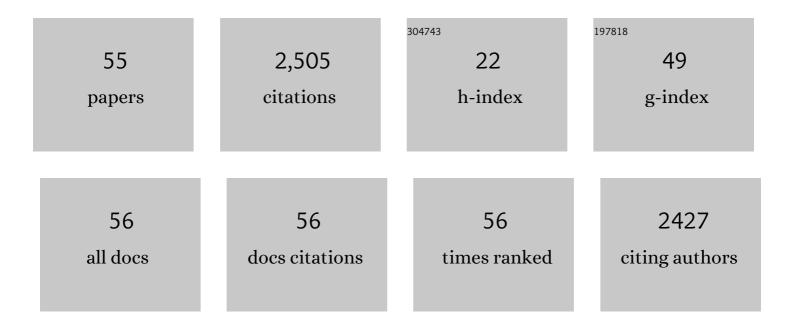
Bingcheng Luo

List of Publications by Year in descending order

Source: https://exaly.com/author-pdf/7621095/publications.pdf Version: 2024-02-01



RINCCHENC LUO

#	Article	IF	CITATIONS
1	Central metal and ligand effects on oxygen electrocatalysis over 3d transition metal single-atom catalysts: A theoretical investigation. Chemical Engineering Journal, 2022, 427, 132038.	12.7	65
2	A Review on the Conventional Capacitors, Supercapacitors, and Emerging Hybrid Ion Capacitors: Past, Present, and Future. Advanced Energy and Sustainability Research, 2022, 3, .	5.8	74
3	Novel atomic-scale graphene metamaterials with broadband electromagnetic wave absorption and ultra-high elastic modulus. Carbon, 2022, 196, 146-153.	10.3	9
4	A triatomic carbon and derived pentacarbides with superstrong mechanical properties. IScience, 2022, 25, 104712.	4.1	6
5	Superhierarchical Inorganic/Organic Nanocomposites Exhibiting Simultaneous Ultrahigh Dielectric Energy Density and High Efficiency. Advanced Functional Materials, 2021, 31, 2007994.	14.9	46
6	Electronic, structural and optical properties of cerium and zinc co-doped organic-inorganic halide perovskites for photovoltaic application. Physica B: Condensed Matter, 2021, 603, 412703.	2.7	4
7	Layered Nanosheets: Superhierarchical Inorganic/Organic Nanocomposites Exhibiting Simultaneous Ultrahigh Dielectric Energy Density and High Efficiency (Adv. Funct. Mater. 8/2021). Advanced Functional Materials, 2021, 31, 2170050.	14.9	5
8	Structural and Electronic Engineering of Ir-Doped Ni-(Oxy)hydroxide Nanosheets for Enhanced Oxygen Evolution Activity. ACS Catalysis, 2021, 11, 5386-5395.	11.2	75
9	Electronic structure and optical properties of SnO2/HC(NH2)2PbI3 interfaces from first-principles calculations. Surfaces and Interfaces, 2021, 23, 100913.	3.0	3
10	Structural, electronic, and optical properties of two-dimensional hafnium monoxide nanosheets. Physica E: Low-Dimensional Systems and Nanostructures, 2021, 130, 114690.	2.7	3
11	Multiphase Engineered BNT-Based Ceramics with Simultaneous High Polarization and Superior Breakdown Strength for Energy Storage Applications. ACS Applied Materials & Interfaces, 2021, 13, 28484-28492.	8.0	52
12	Ferroelectric properties of BaTiO3-BiScO3 weakly coupled relaxor energy-storage ceramics from first-principles calculations. Journal of Alloys and Compounds, 2021, 866, 158933.	5.5	17
13	Vortex domain configuration for energy-storage ferroelectric ceramics design: A phase-field simulation. Applied Physics Letters, 2021, 119, .	3.3	13
14	High temperature lead-free BNT-based ceramics with stable energy storage and dielectric properties. Journal of Materials Chemistry A, 2020, 8, 683-692.	10.3	167
15	Enhanced near-ultraviolet and visible light absorption of organic-inorganic halide perovskites by co-doping with cesium and barium: Insight from first-principles calculations. Journal of Solid State Chemistry, 2020, 289, 121477.	2.9	4
16	Tailoring the Dimension of Halide Perovskites Enables Quantum Wires with Enhanced Visible Light Absorption. Journal of Physical Chemistry C, 2020, 124, 11124-11131.	3.1	1
17	Thermally stimulated relaxation and behaviors of oxygen vacancies in SrTiO ₃ single crystals with (100), (110) and (111) orientations. Materials Research Express, 2020, 7, 046305.	1.6	3
18	Graphene-like monolayer monoxides and monochlorides. Proceedings of the National Academy of Sciences of the United States of America, 2019, 116, 17213-17218.	7.1	54

BINGCHENG LUO

#	Article	IF	CITATIONS
19	Interfacial Bonding and Electronic Structure between Copper Thiocyanate and Hybrid Organohalide Lead Perovskites for Photovoltaic Application. Journal of Physical Chemistry Letters, 2019, 10, 5609-5616.	4.6	4
20	Interfacial electronic properties of ferroelectric nanocomposites for energy storage application. Materials Today Energy, 2019, 12, 136-145.	4.7	23
21	Core-shell structure-induced high displacement response in piezoelectric ceramics: A theoretical design. Ceramics International, 2019, 45, 8940-8944.	4.8	2
22	Enhanced temperature stability of electric-field-induced strain in KNN-based ceramics. Journal of Alloys and Compounds, 2019, 786, 498-506.	5.5	9
23	Homogeneity quantification of nanoparticles dispersion in composite materials. Polymer Composites, 2019, 40, 1000-1005.	4.6	4
24	Laminated structure-induced high dielectric strength and energy storage density in dielectric composites. Composites Science and Technology, 2019, 173, 61-65.	7.8	7
25	Mechanism of ferroelectric properties of (BaCa)(ZrTi)O3 from first-principles calculations. Ceramics International, 2018, 44, 9684-9688.	4.8	10
26	Enhancement of strain by electrically-induced phase transitions in BNKT-based ceramics. Journal of Alloys and Compounds, 2018, 744, 535-543.	5.5	18
27	Chemical composition and temperature dependence of the energy storage properties of Ba _{1â€} <scp>_xS</scp> r _x TiO ₃ ferroelectrics. Journal of the American Ceramic Society, 2018, 101, 2976-2986.	3.8	24
28	Giant permittivity and low dielectric loss of Fe doped BaTiO3 ceramics: Experimental and first-principles calculations. Journal of the European Ceramic Society, 2018, 38, 1562-1568.	5.7	54
29	Hierarchical-structured dielectric permittivity and breakdown performances of polymer-ceramic nanocomposites. Ceramics International, 2018, 44, 843-848.	4.8	15
30	The properties of Al ₂ O ₃ coated fineâ€grain temperature stable BaTiO ₃ â€based ceramics sintered in reducing atmosphere. Journal of the American Ceramic Society, 2018, 101, 1245-1254.	3.8	32
31	Multiscale design of highâ€voltage multilayer energyâ€storage ceramic capacitors. Journal of the American Ceramic Society, 2018, 101, 1607-1615.	3.8	31
32	Influence of Fe doping on the crystal structure, electronic structure and supercapacitance performance of birnessite [(Na, K)x(Mn4+, Mn3+)2O4·1.5H2O] with high areal mass loading. Electrochimica Acta, 2018, 291, 31-40.	5.2	17
33	Grainâ€size–dependent dielectric properties in nanograin ferroelectrics. Journal of the American Ceramic Society, 2018, 101, 5487-5496.	3.8	121
34	Electronic, dielectric and optical properties of orthorhombic lanthanum gallate perovskite. Journal of Alloys and Compounds, 2017, 708, 187-193.	5.5	16
35	Thermal mismatch strain induced disorder of Y ₂ Mo ₃ O ₁₂ and its effect on thermal expansion of Y ₂ Mo ₃ O ₁₂ /Al composites. Physical Chemistry Chemical Physics, 2017, 19, 11778-11785.	2.8	16
36	Enhanced Energy-Storage Density and High Efficiency of Lead-Free CaTiO ₃ –BiScO ₃ Linear Dielectric Ceramics. ACS Applied Materials & Interfaces, 2017, 9, 19963-19972.	8.0	145

BINGCHENG LUO

#	Article	IF	CITATIONS
37	Interfacial electronic and structural properties of SiO2(010)/BaTiO3(001) from first-principles calculations. Ceramics International, 2017, 43, 12988-12991.	4.8	4
38	Dielectric response and breakdown behavior of polymer-ceramic nanocomposites: The effect of nanoparticle distribution. Composites Science and Technology, 2017, 145, 105-113.	7.8	86
39	Nanocomposites with enhanced dielectric permittivity and breakdown strength by microstructure design of nanofillers. Composites Science and Technology, 2017, 151, 109-114.	7.8	34
40	P(VDF-HFP)/PMMA flexible composite films with enhanced energy storage density and efficiency. Composites Science and Technology, 2017, 151, 94-103.	7.8	93
41	Thermal-mechanical-electrical coupled design of multilayer energy storage ceramic capacitors. Ceramics International, 2017, 43, 12882-12887.	4.8	8
42	Reâ€entrant relaxor behavior in BaTiO ₃ â€Bi(Zn _{2/3} Nb _{1/3})O ₃ ceramics. Journal of the American Ceramic Society, 2017, 100, 511-514.	3.8	11
43	Influence of BaO-CaO-SiO ₂ on dielectric properties and reliability of BaTiO ₃ -based ceramics. Physica Status Solidi (A) Applications and Materials Science, 2016, 213, 1077-1081.	1.8	6
44	Dielectric, ferroelectric, and thermodynamic properties of silicone oil modified PVDF films for energy storage application. Applied Physics Letters, 2016, 108, .	3.3	6
45	First-principles effective Hamiltonian simulation of ABO3-type perovskite ferroelectrics for energy storage application. Journal of Applied Physics, 2016, 120, 074106.	2.5	11
46	Dielectric Enhancement in Graphene/Barium Titanate Nanocomposites. ACS Applied Materials & Interfaces, 2016, 8, 3340-3348.	8.0	47
47	Synthesis, characterization and dielectric properties of surface functionalized ferroelectric ceramic/epoxy resin composites with high dielectric permittivity. Composites Science and Technology, 2015, 112, 1-7.	7.8	80
48	Electronic structure, optical and dielectric properties of BaTiO ₃ /CaTiO ₃ /SrTiO ₃ ferroelectric superlattices from first-principles calculations. Journal of Materials Chemistry C, 2015, 3, 8625-8633.	5.5	96
49	BaTiO ₃ –BiYbO ₃ perovskite materials for energy storage applications. Journal of Materials Chemistry A, 2015, 3, 18146-18153.	10.3	393
50	Structural and electronic properties of cubic KNbO3 (001) surfaces: A first-principles study. Applied Surface Science, 2015, 351, 558-564.	6.1	14
51	Electronic structure, elastic and thermal properties of semiconductor GaX (X = N, P, As, Sb) with zinc blende from first-principles calculation. International Journal of Modern Physics B, 2014, 28, 1450183.	2.0	7
52	Composition and ionic change capacity variation of surfactant-intercalated MgFe-layered double hydroxides in the one step synthesis. Journal of Sol-Gel Science and Technology, 2014, 69, 26-32.	2.4	6
53	Fabrication, characterization, properties and theoretical analysis of ceramic/PVDF composite flexible films with high dielectric constant and low dielectric loss. Journal of Materials Chemistry A, 2014, 2, 510-519.	10.3	375
54	Effect of final pyrolysis temperature on the mechanical and thermal properties of carbon foams reinforced by aluminosilicate. Materials Science & Engineering A: Structural Materials: Properties, Microstructure and Processing, 2012, 558, 446-450.	5.6	10

#	Article	IF	CITATIONS
55	Preparation and characterization of carbon foams derived from aluminosilicate and phenolic resin. Carbon, 2011, 49, 1782-1786.	10.3	61